DYNAMICS OF SINGLE CHAINS OF SUSPENDED FERROFLUID PARTICLES.

S. Cutillas and J. Liu, California State University Long Beach, Department of Physics and Astronomy,
1250 Bellflower Boulevard, 90840 CA, Long Beach.

Introduction

Super paramagnetic particles is a new class of magnetic materials that exhibit a susceptibility χ near the value of one while most of natural paramagnetic materials have a magnetic susceptibility at least five orders of magnitude lower. Ferrofluid emulsion is one of such systems. A collection of iron oxide nanoparticles (in our case Fe_3O_4 with a radius of 6nm) dispersed in kerosene is called a ferrofluid which has various properties [1]. The most important is that each nanoparticle has a permanent dipole moment. Due to the small size of the nanoparticles, they only have a single domain magnetization. The thermal agitation randomizes the iron oxide particles so that the total magnetization of the ferrofluid is equal to zero when no magnetic field is applied. Once an external magnetic field is applied, the nanoparticles are oriented slightly in the field direction and the ferrofluid can have a strong magnetization. Particles, having a submicronic size, (in our case 0.23μm as radius) can be made of this ferrofluid. If these ferrofluid droplets are dispersed in water, some surfactant is added to prevent aggregation, the system thus produced is called a ferrofluid emulsion.

When ferrofluid particles are suspended in water, they diffuse under Brownian forces. Applying a magnetic field to such a suspension leads to dipole-dipole interactions between particles. The amplitude of this interaction is described by a dimensionless parameter λ, which is the ratio of the magnetic dipolar energy over the thermal energy [2]:

$$\lambda = \frac{\pi a^3 \chi^2 \mu_0 H_0^2}{18kT} \qquad (1)$$

Where a is the particle radius, μ_0 is the vacuum permeability, H_0 the applied magnetic field, k the Boltzmann constant and T the absolute temperature. When λ is greater than one, magnetic interactions dominate. Because of the strong anisotropy of the dipolar interaction, particles aggregate to form chains in the field direction (cf. Fig.1).

Low fields $\lambda \ll 1$ High fields $\lambda > 1$
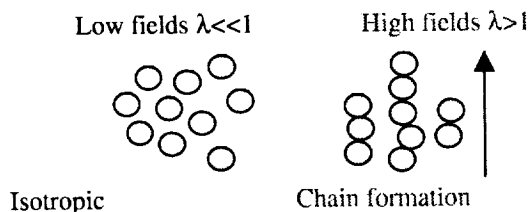

Isotropic   Chain formation

Figure 1: Magnetic field effect on a ferrofluid emulsion.

When the volume fraction is high, bigger aggregates are formed by the lateral coalescence of several chains [3,4,5]. While many studies and applications deal with the rheological properties [6] or the field-induced structural changes [3-7], this work is to better understand the chain dynamics. We will show, in the first section, that the kinetics of chain formation is a diffusion-limited aggregation. The second and the main part of this work will talk about measurements of the effective diffusion coefficient by dynamic light scattering (DLS) [8]. In particular, our experiments are able to measure two different motions. One is from the center of mass of the chain and the other is from internal motions (particle fluctuations). This is an extension of our earlier work [9,18].

Experimental conditions

Our sample consists of ferrofluid particles dispersed in water. The particle volume fraction is 10^{-5} to avoid multiply scattering as well as chain-chain lateral aggregation. The emulsion is introduced in a test tube of 2cm of diameter with care to avoid dust pollution.

scattering vector q:
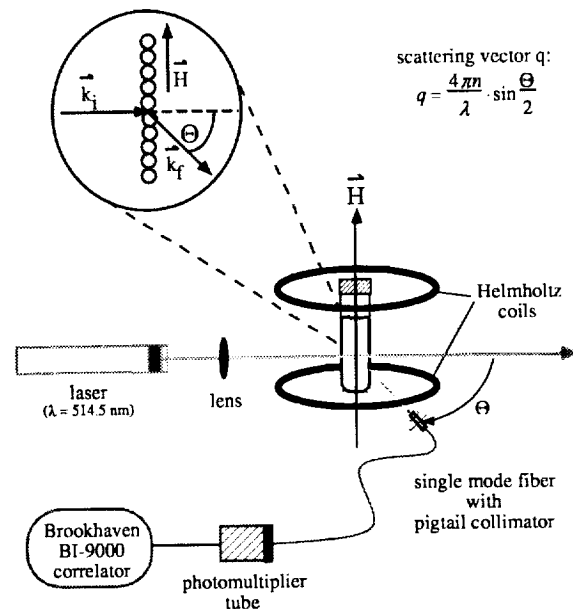$$q = \frac{4\pi n}{\lambda} \cdot \sin\frac{\Theta}{2}$$

Figure 2: Experimental setup of dynamic light scattering. The onset specifies our scattering geometry, with

chains perpendicular to the scattering plane, and the definition of q is also indicated.

The tube is placed in the sample holder with an index match bath to reduce reflections. The sample holder is then put inside a pair of Helmholtz coils as shown in Fig.2.

An Ion Argon laser beam (λ_0=514.5nm) is focused through a lens (with a focal length equal to 25cm) to the sample. The detector is placed at an angle θ from the initial path that specifies the momentum transfer q, defined in the experimental setup shown in Fig.2. The scattered light is collected by a photomultiplier tube and analyzed by a digital correlator to give the intensity autocorrelation function. In self beating mode, often called homodyne mode, the intensity autocorrelation function that the correlator measures $<I(q,t)I(q,0)>$ is related to the dynamic structure factor $S(q,t)$ with the relation:

$$< I(q,t)I(q,0)>-<I^2>=\alpha S^2(q,t) \quad (2)$$

And

$$S(q,t)=\frac{1}{V}\sum_{n,p}\exp\left\{iq(r_n(t)-r_p(0))\right\} \quad (3)$$

$<I^2>$ is the mean square amplitude of the intensity and α is a parameter that only depends on geometrical factors. V is the scattering volume and $r_n(t)$ is the position of the particle number n at time t. In general, interpretation of DLS experiments requires a model for $S(q,t)$.

In the absence of magnetic field, the suspension is isotropic without any interactions between particles and the structure factor reduces to a single exponential $S(q,t)\propto exp(-q^2D_0t)$. $D_0=(kT/\xi)$ is the diffusion coefficient of a particle. $\xi=6\pi\,\eta\,a$ is the Stokes frictional coefficient of a spherical particle in a fluid of viscosity η. If interactions or polydispersity can not be ignored, an effective diffusion coefficient has to be introduced. Formally, D_{eff} is defined as:

$$D_{eff}=-\frac{1}{q^2}\frac{\partial}{\partial t}\ln(S(q,t))\Big|_{t\to0}$$

It reduces to D_0 if no interactions between particles are present. Therefore, without magnetic field, we can use DLS to measure particle size. The particle radius was found to be $a=0.23\mu$ m with 7% of polydispersity through a fitting procedure called cumulant expansion [8]. In this case, if we vary the scattering angle θ (and so q) we do not have any change in the measured diffusion coefficient: it is q-independent.

When a magnetic field is applied, the system consists of particles and chains. Equation 2 can still be used to fit our data if we assume $S(q,t)\sim exp(-\Omega\ t)$ and

$\Omega\ =q^2D_{eff}$. Ω measures the frequency of scatters (particles, chains).

The magnetic field is controlled by a computer (with a digital-analog converter board) connected to a remote power supply. The field was first calibrated without any magnetic material and a linear relation between the current and the field was found. Each Amp produces 67.0±0.5 Gauss. The relation giving λ for a given magnetic field strength is not simple since the susceptibility varies with the magnetic field. However, an order of magnitude can be found with the equation λ=0.01B^2, where B is the external magnetic field applied, expressed in Gauss. For 200Gauss, λ=400. Our expressions of λ, given in this paper, are rigorous solutions of the equations of the magnetic field in heterogeneous media.

Results

I) Kinetics of chain formation

When a strong magnetic field is applied (λ=406), at a fixed q, we first notice a monotonous decrease of the effective diffusion coefficient with time. Physically, this means that chains are becoming longer and longer with time (see Fig.3).
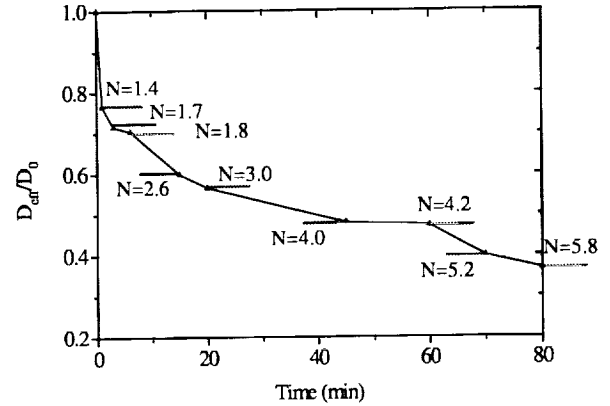

Figure 3: Normalized effective diffusion coefficient versus time. (λ=406, q= 4.2x10^6 m^{-1})

To obtain chain length from D_{eff}, a theoretical model of rigid chains of N spherical particles is used [11,12] since it agrees very well with a recent experiment [10]. The result is shown below:

$$D_{chain}=f(N)D_0$$

$$f(N)=\frac{3\ln(2N)+1.254}{4N} \quad (4)$$

Here, we assume that the effective diffusion coefficient measures the average motion of isolated chains. In very dilute system like the one we used, this is cer-

tainly true. From equation 4, we are able to get the mean number of particles per chain, N, from the effective diffusion coefficient.

This is illustrated in the Fig.4 where the effective diffusion coefficient is normalized by that of a single particle. Figure 4 shows a Log-Log plot of the results based on measurements of Fig.3.

Calculating the value of N as a function of the time gives us information about the kinetics of aggregation (i.e. N versus time).
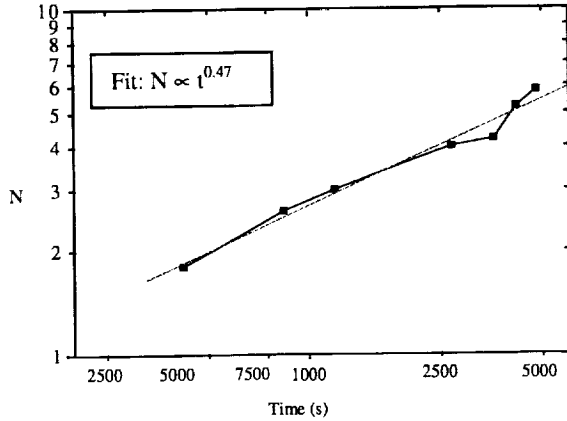

Fit: $N \propto t^{0.47}$

Figure 4: Mean number of particle per chain versus time, kinetics of chain formation.

Fitting the data with a power-law relation gives an exponent of 0.47±0.05. Thus, N depends on time as a square root (within our experimental uncertainties for this short chain formation). As expected, since the volume fraction is very low, the kinetics of particle aggregation into chains is a diffusion-limited aggregation. This is consistent with our earlier data and other work [9,18,13].

II) Dynamics of single chains

If we apply a magnetic field of 200 G to the sample for 6 hours, we can get chains long enough (more than 19 particles) and far away (more that 70 particle diameters) that the chain growth slow down. Now, we can do other experiments. In this case, the absolute time is no longer important since chain length is almost constant during the next 30 minutes. First, we vary θ (or q) at a constant magnetic field strength, and measure the effective diffusion coefficient.

Varying q allows us to select a window within which different length scales of motion will be probed. This can be seen in another way: q defines a characteristic length ($l=2\pi/q$) over which dominantly motion will contribute to the intensity correlation function. To be able to probe different length scales by

varying the scattering angle is an important property of DLS.

In this work, the experimental range of the scattering angle is $5° < \theta < 130°$. The equivalent range for the scattering wave vector is $1.4\times10^6 < q(m^{-1}) < 2.9\times10^7$. Thus, the characteristic length scale will have the range $0.21 < l$ (μm) < 4.42. In terms of the particle radius:

$$0.9a < l < 20a. \qquad (5)$$

We can see here that motions will be probed over quite a broad range in a single experiment from one particle radius up to twenty particle radii.

Next, we vary the magnetic field intensity (or λ) and repeat the q-dependence experiment.

Figure 5 shows four series of experiments performed at different magnetic field or coupling constant λ (indicated in the onset). To work with the same chain length, these four experiments are done consecutively after the 6 hours at $\lambda=406$. The first one is for $\lambda=406$, the second one is for $\lambda=17$, the third one is for $\lambda=157$ and the last one is for $\lambda=46$. Each experiment takes around 30 minutes. This procedure allows us first to decrease the magnetic energy of interaction between chains to slow down again the kinetics of aggregation and second to cool the coils which were warm after a long-time experiment. At each fixed λ value, we measure the effective diffusion coefficient D_{eff} as a function of q. D_{eff} is normalized by the single particle diffusion coefficient D_0, and $l=2\pi/q$ is normalized by the particle radius a.
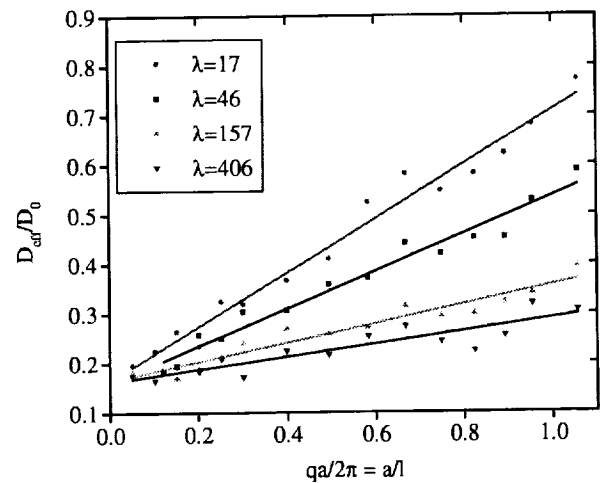

Figure 5: Dependence of the normalized effective diffusion coefficient versus the normalized scattering wave vector for different λ values.

Figure 5 shows a few interesting features. First, for all λ values, D_{eff} is linearly proportional to qa. Second,

as λ increases the slope of D_{eff} versus q decreases. But all these straight lines converge to the same point $(D_{eff}/D_0=0.16)$ as q approaches zero.

To understand the q dependency of D_{eff}, let us look at the probing length used. In our study, the characteristic length scale probed is $l=2\pi/q$ which is in the range of $0.9<l/a<20$. When l is much larger than the particle radius $(l/a \to \infty)$ we are mainly sensitive to the center of mass diffusion of the chain. D_{eff} is then the diffusion of the entire chain and depends only on N and D_0 but not on q and λ. The value D_{eff} allows us to obtain the number of particles per chain N. In the opposite limit (i.e. $l/a<1$), we are sensitive to motions on the size of individual particles. The main contributions to the measured diffusion coefficient come from internal motions of the chains (i.e. particles' fluctuations inside the chain). However, the reason for a linear dependence of D_{eff} on q is not clear.

The fact that the initial value of D_{eff}/D_0 (here equal to 0.16 when q approaches zero) does not depend on λ indicates that the straight chain configuration is well maintained even for the lowest λ values we used. This value can be used to find the number of particles per chain from the equation (4). This gives us $N=19\pm1$ as the mean number of particles in a chain (after 6 hours at $\lambda=406$).

Figure 6 shows the dependence of D_{eff} on λ based on the data in Fig.5. Since $D_{eff}/D_0\sim k(qa)$, we plotted, in a Log-Log plot, the slope k versus λ in Fig.6. Here, a fit of power-law is obtained $D_{eff}/D_0 \propto \lambda^\delta$ giving the exponent $\delta = -0.47\pm0.05$.
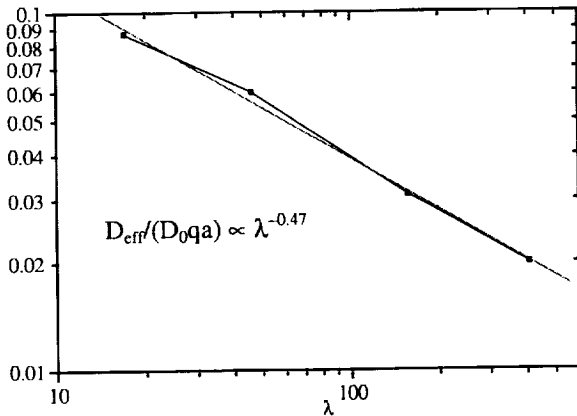

$$D_{eff}/(D_0qa) \propto \lambda^{-0.47}$$

Figure 6: Slope of the curves shown in Fig.5 as a function of λ to obtain power law dependence.

We can approximate $D_{eff}/D_0\sim1/\sqrt{\lambda}$. We can see here that when the magnetic field increases (so λ increases) this reduces the internal motions. Therefore, based on the results of Fig.5 and 6, D_{eff}/D_0 may be written as:

$$D_{eff}/D_0 = \frac{A}{\sqrt{\lambda}}g(N)qa + f(N) \quad (6)$$

This effective diffusion coefficient given by Eq.6 is consisted of two parts.

The first term is the contribution due to internal motions of the chain (particle fluctuations) while the second part is due to the whole chain motion (diffusion of the center of mass of the chain).

In Eq.6, $g(N)$ accounts for the chain length dependence. $g(N)$ and the constant A is determined from experiments described below.

We created two chain lengths to study the effect of chain length on the effective diffusion coefficient. To obtain a longer chain size than 19 particles per chain, we hold the magnetic field at $\lambda=406$ for 3 more hours (this increases the experimental time up to more than 9 hours). We then reduced the field down to $\lambda=46$ and repeated the q-dependence measurements. The result is shown in Fig.7 below where for the same value of λ $(\lambda=46)$ two experiments with two different chain sizes are compared here:
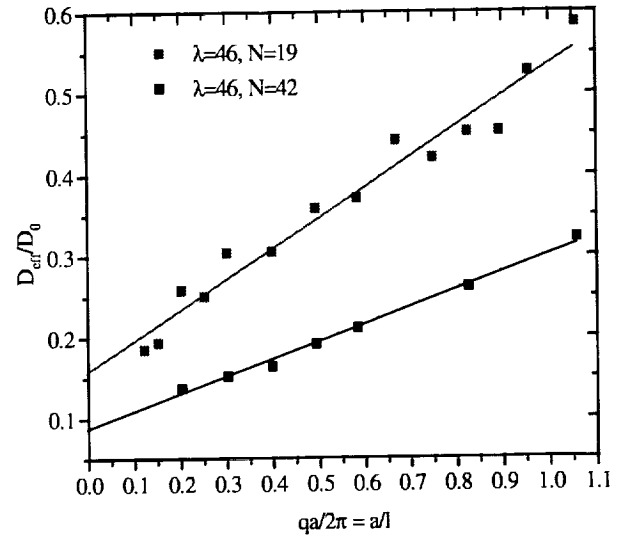
Figure 7: Effect of different chain sizes on the meas-

$qa/2\pi = a/l$

ured diffusion coefficient versus q.

From the data shown in Fig.7, we notice that when N varies, not only the initial value is different but also the slope changes. If we also assume that $D_{eff}/D_0 \propto N^\varepsilon$, ε is found to (-0.7 ± 0.1).

To summarize the results from figures 5,6 and 7, we found that the effective diffusion coefficient follows the simple relation:

$$D_{eff}/D_0 = \frac{3}{N^{0.7}\sqrt{\lambda}}qa + f(N) \quad (7)$$

Here $f(N)$ is given by equation 4. The constant A was found equal to 3.0 ± 0.2. It was determined experi-

mentally by finding the exact value of D_{eff}/D_0 from Fig.5 for a given $qa/2\pi$.

It is worth noting here that our experiments do not cover the whole range of probing window $(1=2\pi /q)$. We were only sensitive to the most interesting range where a q dependency of D_{eff} can be observed. However, if we expand the q range toward both ends, different behavior of D_{eff} may be observed. Based on dynamics of polymers [14,15], we expect a qualitative behavior as shown in the Fig.8. Here, three dynamical regimes exist.

For small qa values, D_{eff}/D_p corresponds to the diffusion coefficient of the entire chain. In the opposite limit $(qa>2\pi)$ it corresponds to the diffusion coefficient of the monomer inside a polymer chain D_p.
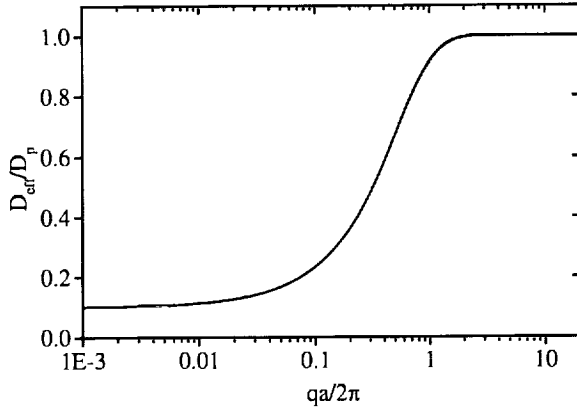

Figure 8: Universal behavior of the effective diffusion coefficient versus q in polymer physics.

In our case D_p is the diffusion coefficient of a single particle in the chain configuration. Notice that D_p is different from the case of isolated particles D_0. In both of these regions, the behavior of D_{eff}/D_p does not depend on $qa/2\pi$. If a broader range of $qa/2\pi$ was accessible we expect to see also these two others regions where D_{eff}/D_0 becomes constant.

In our experiment, the characteristic frequency [15] probed by DLS is defined as Ω $(q)=D_{eff}q^2$.

$$\Omega(q) = \left[\frac{3}{N^{0.7}\sqrt{\lambda}} qa + f(N) \right] q^2 D_0 \qquad (8)$$

The two constant regions can be obtained by setting $qa=0$ and $qa=2\pi$. When $qa=0$, $D_{eff}=D_{chain}$ or, in terms of the minimum frequency, $\Omega_{min}=q^2 D_{chain}$. When $qa/2\pi$ approaches 1, the maximum frequency is obtained by replacing qa by 2π in Eq.7 for the effective diffusion coefficient. The result, valid for $q>(2\pi /a)$, is:

$$\Omega_{max}(q) = (\frac{6\pi}{N^{0.7}\sqrt{\lambda}} + f(N)) q^2 D_0 \qquad (9)$$

In this work, we just reached the boundary of the two limits. If we extend qa a little large, we may see the saturation behavior. From equations (7, 8 and 9) we can see that the higher λ and N are, the lower the internal vibration frequency and the slower the diffusion motion. Increasing the magnetic interaction leads to a more rigid chain, which is reasonable. Decreasing λ reduces the dipolar binding between particles in a chain. Thus, fluctuations of higher frequency are observed. However, λ can not be reduced below the value of 1. In this case, only the motion of isolated particles will be probed (if no irreversible aggregation occurred) since chains break [16]. The N dependence indicates that when the number of particles per chain increases, internal frequencies of the chain reduce. This behavior may be explained by the fact that more vibrational modes are present for a longer chain than that of a shorter chain. If the slowest modes (or the longest wavelength) contribute mainly to the probed fluctuations, the characteristic frequency will decrease with chain length.

For $N>5$, $f(N)\approx (3/2)N^{0.75}$. Therefore, we may replace $N^{0.7}$ in Eq.6-9 by $f(N)$. Thus, equation (7) becomes:

$$D_{eff} \approx (\frac{2}{\sqrt{\lambda}} qa + 1) f(N) D_0 \qquad (10)$$

We can write Eq.10 by separating the two parts. The internal part with an apparent internal diffusion coefficient D_{int}, and the global part with the diffusion coefficient of the whole chain D_{chain}.

$$D_{eff} = D_{int} + D_{chain}$$

With

$$D_{int} = \frac{2qa}{\sqrt{\lambda}} D_{chain} \quad \text{and} \quad D_{chain} = f(N) D_0$$

Equations (8) and (9) can also be expressed in a closed form:

$$\Omega(q) = (\frac{2}{\sqrt{\lambda}} q^3 a + q^2) f(N) D_0 \qquad (11)$$

And, for $q>(2\pi /a)$:

$$\Omega_{max}(q) = (\frac{4\pi}{\sqrt{\lambda}} + 1) f(N) q^2 D_0 \qquad (12)$$

The apparent diffusion coefficient of particles in a chain configuration D_p is given in terms of the maximum frequency (term "apparent" is used since a particle does not have a real diffusion behavior inside a chain because of its bounding motion):

$$D_p = \frac{\Omega_{max}}{q^2} = (\frac{4\pi}{\sqrt{\lambda}} + 1) D_{chain} \qquad (13)$$

From equation (13) we see that D_p reduces to D_{chain} when $\lambda>>(4\pi)^2 =160$ and that the particle radius is completely contained in the single particle diffusion

coefficient D_0. Because of the square root dependence, even in the case $\lambda=10^4$, internal fluctuations still contribute f 12% of that of the whole chain. To reach $D_{int}/D_{chain} = 1\%$, $\lambda=10^6$ is necessary. In practice, such a large λ value is difficult to obtain with submicronic particles, due to saturation of magnetization. In our case, if no saturation effect is taken account, the magnetic field would have the value of 1 Tesla to get a completely rigid chain. In our case, for the maximum magnetic field used, $\lambda=406$ and $D_{int}/D_{chain} = 62\%$.

Physically, this means that in almost all experiments realized with these systems composed of submicronic super-paramagnetic particles, chain fluctuations can not be neglected. Furthermore, the only way to obtain rigid chains is to increase the particle size well above the micrometer. Since the magnetic interactions is proportional to the cube of the particle radius (cf. Eq.1), a particle diameter about 3 micrometers need to be used with a magnetic field of 300 Gauss to reach $\lambda=10^6$ (assuming the same magnetic susceptibility). The biggest problem with such particles will be their sedimentation and stability of ferrofluid droplets. Furthermore, using these particles we can test if rigid chains coalesce into bigger aggregate as theoretical prediction suggested [17]. This is our next project.

Conclusion

In conclusion, we find that DLS is a powerful technique in probing the dynamics of chains. We made quantitative measurements concerning the variation of our parameters; the coupling parameter λ, the mean number of particles per chain N and the particle radius a. For instance, we showed that the frequency of the fluctuations depend on the magnetic interaction through $1/\sqrt{\lambda}$ (the higher the field, the more rigid the chain). The dependence of the number of particle per chain also leads to slow down the characteristic frequency when the chain length increases.

We found separated motions when the scattering wave vector varies. The effective diffusion coefficient comprises two parts. The first one comes from the diffusion of the center of mass of the chain (drift motion), and the second one comes from the internal fluctuations of particles that compose the chain. These internal fluctuations can not be neglected even for the highest magnetic field used in our experiments ($\lambda=406$, $D_{int}/D_{chain}=62\%$). This work is a basic study of the chain dynamics. It is the first step leading to a better understanding the mechanism of chain-chain lateral aggregation in the field-induced structural formation of dipolar fluids.

Acknowledgements

References

[1.] R.E. Rosensweig, Ferrohydrodynamics, Cambridge University Press, 1985.

[2.] P.G. de Gennes & P.A Pincus. (1970), Phys Kondens Mat., 11, 189.

[3.] G.A. Flores, J. Liu, M. Mohebi & N. Jamasbi, "Field induced columnar and bent-wall-like patterns in a ferrofluid emulsion", proceeding of the 6th international conference on E.R.F. & M.R.S &A.T. Japan (1997) To be published.

[4.] J. Liu et al, "Field-Induced Structures in Ferrofluid Emulsions", Phys. Rev. Letters, 74 (14), p. 2828 (1995).

[5.] S. Cutillas and G. Bossis, "A comparison between flow-induced structures in electro- and magneto-rheological fluids", Europhys. Lett., 40 (4), 465 (1997).

[6.] E. Lemaire et al, "Influence of the particle size on the rheology of magnetic suspensions", J of Rheology, 39(5), (1995)

[7.] S. Cutillas, G. Bossis and A. Cebers, "Flow-Induced transition from cylindrical to layered patterns in MR fluids" Phys Rev E, 57 (1), 804, (1998).

[8.] B.J. Berne & R. Pecora, Dynamic Light Scattering, Wiley and Sons, New York, (1966).

[9.] M. Hagenbuechle and J. Liu, "Study of chain formation and chain dynamics in a dilute magneto-rheological fluid", Applied Optics, 36, p. 7664, (1997).

[10.] K. Zhan, R. Lenke and G. Maret, J. Phys. II France, 4, p. 555, (1994)

[11.] H. Yamakawa, Transport properties of polymer chains in dilute solution: hydrodynamic interactions, J. Chem. Phys., 53, p.436, (1970).

[12.] G. K. Batchelor, "Slender-body theory for particles with arbitrary cross-section in Stokes flow", J. Fluid. Mech., 44, p.419, (1970).

[13.] M. Fermigier & A.P. Gast, "Structure Evolution in a Paramagnetic Latex Suspension", J. Coll. Int. Sci., 154, 522, (1992).

[14.] R. Pecora, Dynamic Light Scattering, Plenum Press, New York (1985).

[15.] P. G. de Gennes, Scaling concepts in polymer physics, Cornell University Press (1979)

[16.] S. Cutillas, G. Bossis, E. Lemaire, A. Meunier and A. Cebers, "Experimental and theoretical study of the field-induced phase separation in electro- and magnetorheological suspensions", proceeding of the 6th international conference on E.R.F. & M.R.S &A.T. Japan (1997) To be published.

[17.] T. C. Halsey and W. Toor, J. of Stat. Phys., 61, 1257, (1990)

[18.] M. Hagenbuechle and J. Liu, proceeding of the 6th international conference on E.R.F. & M.R.S &A.T. Japan (1997) To be published.